Vibronic coupling and other many-body effects in the $4\sigma_g^{-1}$ photoionization channel of CO_2

P. Roy,[a] R. J. Bartlett, and W. J. Trela
Los Alamos National Laboratory, Los Alamos, New Mexico 87545

T. A. Ferrett,[b] A. C. Parr, S. H. Southworth, and J. E. Hardis
Radiometric and Radiation Physics Divisions, National Institute of Standards and Technology, Gaithersburg, Maryland 20899

V. Schmidt
Fakultät für Physik der Universität Freiburg, D-7800 Freiburg, Federal Republic of Germany

J. L. Dehmer
Argonne National Laboratory, Argonne, Illinois 60439

(Received 24 May 1990; accepted 12 October 1990)

Vibrational branching ratios and photoelectron angular distributions were measured for $4\sigma_g^{-1}$ photoionization of CO_2 in the energy range 20–28 eV. Of particular interest are three vibrational components of the resulting CO_2^+ $\tilde{C}\,^2\Sigma_g^+$ state—the allowed (000) and (100) bands and the forbidden (101) band. The wavelength dependence of the beta parameter for the forbidden band deviated significantly from that of the two allowed bands, showing instead a strong resemblance to that of the $\tilde{B}\,^2\Sigma_u^+$ state. This behavior suggests that vibronic coupling to the $\tilde{B}\,^2\Sigma_u^+$ state is responsible for the appearance of the forbidden (101) band in the $\tilde{C}\,^2\Sigma_g^+$ state photoelectron spectrum. We also observe evidence for other many-body effects—shape-resonance-induced continuum–continuum coupling and doubly excited autoionizing resonances—in the present data.

I. INTRODUCTION

A central challenge of molecular physics is to understand the spectroscopy and dynamics resulting from the interaction of electronic and nuclear motion in molecular fields. A very fruitful approach in recent years has been angle-resolved photoelectron spectroscopy using synchrotron radiation (see, e.g., Refs. 1–3). In these studies, photoabsorption prepares a well-defined dipole-allowed state at a position of interest in the ionization continuum; the resulting photoelectrons carry to the detector detailed information not only on the energy levels of the residual ion but also on the dynamics of the processes occurring between initial photoexcitation and eventual escape of the photoelectron through the molecular field. The conceptual framework for these studies is shaped by the Born–Oppenheimer (BO) and Franck–Condon (FC) approximations,[4] which define successive degrees of independence of the electronic and nuclear motion resulting from their (usually) disparate velocities and energy level spacings. Of particular interest are striking and potentially widespread departures from these approximations, because such departures often lead to a deeper understanding of the dynamics occurring in the excited molecular complex.

Prominent examples of photoionization phenomena that clearly exhibit large departures from the FC and/or BO approximations include shape-resonance-induced non-FC effects, vibrational autoionization, and vibronic coupling in inner-valence spectra. Shape resonances have been found[5–7] to depend sensitively on internuclear separation, causing a strong, nonmonotonic dependence of the dipole amplitude on nuclear coordinates. This causes a breakdown of the FC approximation, which is manifested as non-FC vibrational intensities and v-dependent angular distributions over a spectral range many times the halfwidth of the shape resonance. Vibrational autoionization[8–10] constitutes a breakdown of the BO approximation by definition, its rate depending on the square of $d\mu/dR$, the dependence of the quantum defect of the autoionizing state on internuclear separation. The inner-valence photoelectron spectra of molecules typically exhibit extensive vibronic coupling,[11–15] leading to complex bands of vibronic levels in place of a simple pattern of vibrational progressions associated with a single electronic state. Of course, many other examples of non-BO effects exist in the literature of high-resolution molecular spectroscopy, ion–atom collisions, etc., but the examples cited here serve to illustrate the recent role of molecular photoionization in the present context.

In this paper, we present a new type of evidence for non-BO behavior—the wavelength dependence of photoelectron angular distributions for forbidden vibrational components induced by vibronic coupling—illustrated here for the (101) vibrational component of the CO_2^+ $\tilde{C}\,^2\Sigma_g^+$ state. The presence of such a level may be indicated by a photoelectron angular distribution that differs significantly from those of the other vibrational members of the electronic transition. Indeed, many observations of irregular angular distributions within a vibrational band have been made at fixed photon

[a] Present address: LURE, Orsay 91405, Cedex, France.
[b] Present address: Department of Chemistry, Carleton College, Northfield, Minnesota 55057.

energy, dating to the early measurements by Carlson and coworkers.[16–19] Such irregularities can arise from a number of causes. The important point in the present work is the wavelength dependence of such observations, because, as pointed out by Domcke,[20] such spectral variations can exhibit the signature of the electronic state responsible for the vibronic coupling that causes the forbidden vibration to appear. This approach will be quite generally applicable when the two electronic states involved have different photoelectron angular distributions and should be of growing importance since high-resolution vibrationally resolved photoelectron spectroscopy is now becoming routine with modern synchrotron radiation sources.

II. EXPERIMENTAL METHODS

The apparatus has been described in detail elsewhere.[21] Briefly, the vacuum ultraviolet (VUV) synchrotron radiation emitted from the SURF-II storage ring at the National Institute of Standards and Technology is dispersed by a 2-m normal-incidence monochromator.[22] The monochromatic light beam is channeled by a 2-mm i.d. capillary into the experimental chamber, where it crosses at right angles with an effusive gas jet. The photoelectrons produced are detected by two high-resolution hemispherical electron spectrometers which are equipped with area detectors and positioned at $\theta = 0°$ and 90° with respect to the major axis of polarization of the light.

Measurements were made with the electron spectrometers operating at two pass energies (2 and 5 eV), with good agreement between data sets. The combined resolution of the monochromator light and the electron spectrometers ranged from 36–60 meV and 53–75 meV for the 2-eV and 5-eV pass spectra, respectively, depending on the wavelength and vertical size of the electron beam in the storage ring.

The branching ratios [relative to the $\tilde{C}$ (000) vibronic state] and β parameters were determined by using the expression for the differential cross section in the dipole approximation for a randomly oriented sample ionized with partially linearly polarized light.[21]

$$\frac{d\sigma}{d\Omega} = \frac{\sigma_v(h\nu)}{4\pi}\left[1 + \frac{\beta_v(h\nu)}{4}(3P\cos 2\theta + 1)\right], \quad (1)$$

where P is the degree of linear polarization of the light, θ is the angle between the major polarization axis and the electron ejection direction, and $\sigma_v(h\nu)$ and $\beta_v(h\nu)$ are the partial cross section and asymmetry parameter for the vibronic level v at the photon energy $h\nu$. The energy dependence of the light polarization was determined to be constant by using a triple reflection polarization device.[23] Because the absolute polarization obtained with this device is sensitive to mirror coatings and optical reflectivities, we measured the absolute value of P to be 0.67(2) by calibration with He 1s ionization, with a known β of 2.0. All spectra presented in this work have been corrected for the analyzer transmission functions, which were determined by using measurements on the Ar 3p levels, for which the cross section and β are known.[24] Correction for incident photon flux variations were made by using the photocurrent reading from a tungsten photodiode.

III. BACKGROUND

A. Related studies

The CO_2 molecule has historically attracted a great deal of attention both as a prototype for triatomic molecules and because of its importance in atmospheric, space, plasma, and life sciences. The most relevant studies for the present purposes are the following: Vibronic bands in photoelectron spectra of CO_2 have been observed by HeI photoelectron spectroscopy[18,25–31] and by threshold electron spectroscopy.[32] Angle-resolved photoelectron measurements[18,19,30,33,34] on the $\tilde{C}\,^2\Sigma_g^+$ state of CO_2^+ have revealed that the beta parameter for one forbidden band differs markedly from that of the allowed bands at $h\nu = 584$, 550, and 525 Å. Photoionization of CO_2 exhibits rich shape resonance and autoionization structure. Shape resonances have been the subject of a number of experimental[34–38] and theoretical studies.[36,39–45] For the $4\sigma_g^{-1}$ channel, calculations predict a σ_u shape resonance at a photon energy near 40 eV, beyond the range of the present measurements. Shape resonances in other channels may also enter the picture for $4\sigma_g^{-1}$ photoionization through continuum–continuum coupling.[46–48] Normally interchannel coupling in the continuum is expected to be weak; however, the quasibound nature of shape resonances has been shown to cause transfer of shape resonance character from one ionization continuum to another for $2\sigma_u^{-1}$ photoionization in N_2.[46–48] Autoionization has been observed in absorption,[49–51] total photoionization,[52] and partial cross section measurements[53] in energy regions leading to the $\tilde{X}$, $\tilde{A}$, $\tilde{B}$, and $\tilde{C}$ states of CO_2^+, but not for energies above the $\tilde{C}$ state ionization potential of 19.395 eV.[30]

B. Vibronic coupling

Vibronic coupling can only occur between vibronic states of the ion that have wave functions of the same *total* symmetry.[4] The symmetry of a vibronic state is the direct product of the symmetries associated with the electronic and vibrational states of the ion. The $\tilde{C}$ state electronic symmetry is Σ_g. The symmetries for one quantum of the symmetric stretch (ν_1), bend (ν_2), and asymmetric stretch (ν_3) vibrational modes of CO_2 are Σ_g, Π_u, and Σ_u, respectively, with the symmetric ν_1 mode being the only allowed band for ionization from the symmetric ground state.

In order to consider vibronic coupling involving the (101), (001), (010), and (011) forbidden bands, one must determine the total symmetry for these states and then identify other vibronic states of the same total symmetry. The forbidden band total symmetries are:

$$(101): \Sigma_g(\text{electronic}) \times [\Sigma_g \times \Sigma_u](\text{vibrational}) = \Sigma_u$$
$$(010): \Sigma_g(\text{electronic}) \times \Pi_u(\text{vibrational}) = \Pi_u$$
$$(001): \Sigma_g(\text{electronic}) \times \Sigma_u(\text{vibrational}) = \Sigma_u$$
$$(011): \Sigma_g(\text{electronic}) \times [\Pi_u \times \Sigma_u](\text{vibrational}) = \Pi_g$$

A search for relatively intense vibronic states of the same symmetry yields the following results:

(i) The intensities of the $\tilde{C}(101)$ and (001) bands derive from coupling to the $\tilde{B}\,^2\Sigma_u^+$ $(n00)$ states.

(ii) The $\tilde{C}(010)$ bending mode derives its intensity from coupling with the $\tilde{A}\,^2\Pi_u$ $(n00)$ states.

(iii) The intensity of the $\tilde{C}(011)$ state must result from coupling with the $\tilde{X}\,^2\Pi_g$ $(n00)$ states.

The $\tilde{C}(010)$ bending mode has been assigned to an observed band with binding energy 19.467 eV; we observe this band, but with such weak intensity that quantitative results are not possible. The assignment of the 19.755-eV binding energy peak (observed by us and others) has been controversial, as discussed by Baer and Guyon.[32] These authors and others[28,30,31] favor the (101) assignment, while Domcke[20] and Eland and Berkowitz[26] support (011). Grimm and Larsson[54] suggest the (001) attribution, whereas early work by Carlson and McGuire[18,19] and Brundle and Turner[25] proposed the only symmetry-allowed assignment, (002). Kovac[29] considered both (001) and (002). Without going into exhaustive detail, we believe it is now clear that (101) is the correct assignment for the 19.755 eV peak for the following reasons: First, the ^{13}C isotopic substitution experiment by Baer and Guyon[32] is very strong evidence. Second, evidence presented below shows that only the vibrational frequencies implied by the (101) assignment are compatible with the overtone and combination bands observed at wavelengths of doubly excited autoionizing levels in the present experiment. Third, the (001) assignment implies an unrealistic ν_3, and the (002) assignment does not account for the anomalous β for the 19.755-eV peak. Fourth, the (011) assignment involves a coupling between vibronic states that differ by two nontotally symmetric vibrational species, rather than one. This disobeys a well-known propensity rule for vibronic coupling.[4] Furthermore, this assignment implies intensity borrowing from the $\tilde{X}$ state, which is energetically far removed from the $\tilde{C}$ state.

IV. RESULTS AND DISCUSSION

A. Vibrational level structure and resonant excitation

In Fig. 1, we present photoelectron spectra of CO_2 recorded at a photon energy of 24 eV and at $\theta = 0°$ and 90° relative to the major polarization axis. The four CO_2^+ electronic states $\tilde{X}\,^2\Pi_g$, $\tilde{A}\,^2\Pi_u$, $\tilde{B}\,^2\Sigma_u^+$, and $\tilde{C}\,^2\Sigma_g^+$ appear at binding energies of 13.776, 17.312, 18.074, and 19.395 eV, respectively.[30] Figure 2 is a photoelectron spectrum of the fourth electronic state of CO_2^+, the focus of this study. Four vibrational components are observed at 19.395 eV (000), 19.467 eV (010), 19.550 eV [unresolved (020) and (100)], and 19.755 eV (101). Their intensities and positions are in good agreement with other photoelectron spectra observed at the HeI wavelength.[18,19,25–31] In addition to these peaks, several previously unobserved vibrational peaks in the $\tilde{C}$ state band are resonantly excited in very narrow photon energy ranges, as shown in Table I. There may be even more peaks than those quoted in Table I, since our resolution may not permit separation of all the bands.

We now evaluate several explanations for these resonant bands, including the possibility that experimental artifacts may induce new peaks. First, probable impurity gases (CO, N_2, and O_2) do not have peaks in this binding-energy range. We have ruled out the possibility that second-order light contributes to these new peaks because: (1) we estimate that the second-order light is less than 2–3% for this normal-incidence monochromator in the range of our experiment, (2) the oscillator strength of CO_2 in that energy range further minimizes any disturbance from second-order light,[35,55,56] and (3) the additional peaks do not remain at constant binding energy for ionization by second-order light. A number of other mechanisms are possible. Recent studies[57] have attributed unassigned peaks formed over narrow wavelength ranges to electrons ejected in collisions between target molecules and resonantly excited autoionizing levels of the target gas. For CO_2 the nature of the resonant excitations between 22 and 25 eV are not well enough char-

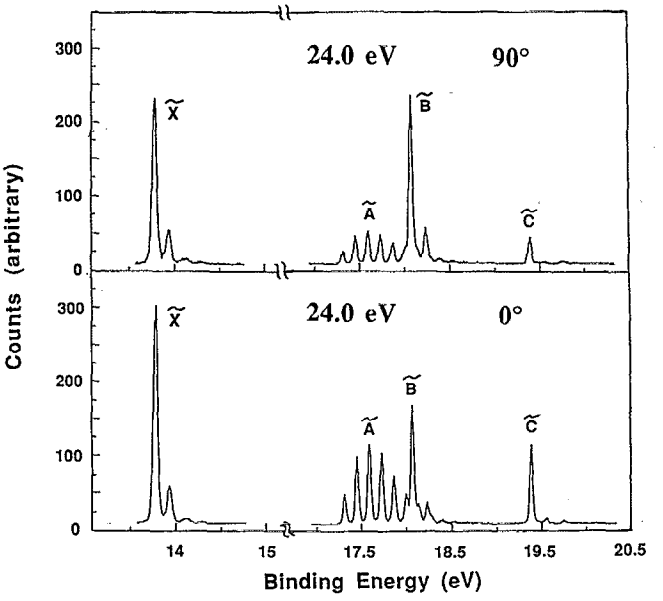

FIG. 1. Photoelectron spectra of CO_2^+ in the 13 to 20.5-eV binding energy range, measured at a photon energy of 24 eV and at $\theta = 0°$ and 90° relative to the major polarization axis of the incident radiation.

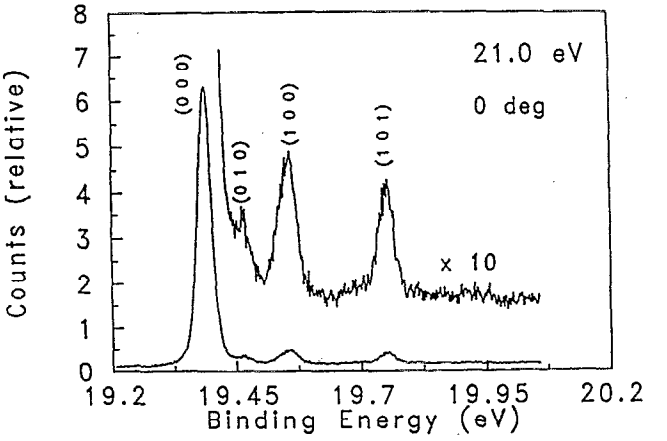

FIG. 2. Photoelectron spectrum of the $\tilde{C}$ state of CO_2^+ measured at a photon energy of 21 eV and at $\theta = 0°$. The forbidden peak of interest appears at 19.755 eV with the (101) attribution.

TABLE I. Binding energies, relative energies, and assignments of the vibrational peaks in the $\tilde{C}$ state of CO_2^+.

Binding energy (eV)	ΔE (meV)	ΔE_{calc} (meV)[a]	Assignment	Photon energy observed (eV)	Vibronic symmetry
19.395[b]	0	-	000	all	Σ_g
19.467	72	-	010	all	Π_u
19.540	145	-	020	all	Σ_g
19.562	167	-	100	all	Σ_g
19.755	360	-	101	all	Σ_u
19.935[c]	540	533,527	102,201	21.218	Σ_g,Σ_u
20.110[c]	715	720	202	21.218	Σ_g
Resonant peaks:[d]					
19.267(8)	−128(8)	-	?	21.90	
19.296(6)	−99(6)	-	?	22.00	
19.31(1)	−85(10)	-	?	22.02	
19.623(8)	228(8)	216	030	23.3	
19.634(8)	239(8)	239	110	23.4	
19.650(8)	255(8)	265	011	23.5	
19.685(8)	290(8)	311,288	120,040	23.6	
19.87(1)	475(10)	478	220	23.75	
19.92(1)	525(10)	527,530	201,022	24.0	
19.84(1)	445(10)	458,432	012,111	24.26	
19.910(7)	515(7)	527,530	201,022	24.5	
20.04(1)	645(10)	651,645	013,320	25.0	

[a] Vibrational assignments are based on an assignment of (101) for the 19.755-eV band, which gives $\nu_3 = 193$ meV, $\nu_1 = 167$ meV, and $\nu_2 = 72$ meV (Ref. 30).
[b] Binding energies taken from Veenhuizen *et al.* (Ref. 30).
[c] Peaks not observed in this study (Ref. 30).
[d] Apparent binding energies from our spectra relative to $\tilde{C}(000)$; photon energies are noted but do not imply the energy of the resonance maxima.

acterized to evaluate this possibility, which, in any event, is less likely than that considered below. Another possibility is that $\tilde{C}(000)$ electrons excite vibrational excitations in CO_2 molecules. This produced the peak at 19.68 eV in an earlier $\tilde{C}$ state spectrum[26] as was later shown in pressure-dependent studies of this spectrum by Reineck *et al.*[28] We, in fact, observe a peak at 19.685 eV binding energy at $h\nu = 23.6$ eV; however, this peak is absent at all other photon energies, indicating that the present measurements are not affected by such pressure effects. We experimentally checked for a pressure dependence of the resonant band at B.E. = 19.634 eV and found the peak intensity to be simply proportional to the pressure. The three peaks to the high kinetic energy (lower apparent binding energy) side of the $\tilde{C}(000)$ lines are especially problematic. The possibility of "hot" bands comes to mind; however, the energy spacings do not correlate well with the vibrational frequencies of CO_2 except for the 85-meV spacing, which does come close to the $\nu_2 = 82.7$ meV interval. This possibility is discounted, however, since these peaks only occur individually at a few selected wavelengths. Another distinct possibility for extra peaks involves excitation of CO_2 molecules by electrons from strong photoelectron peaks, e.g., $\tilde{X}(000)$ and $\tilde{B}(000)$. For example, energy loss of 5.49 eV would cause $\tilde{X}(000)$ photoelectrons to exhibit an apparent binding energy of 19.267 eV, one of the peaks to the high kinetic energy side of the $\tilde{C}(000)$. Insufficient electron energy loss data are available to evaluate this possibility in detail for the present circumstances.

The most straightforward interpretation is that these bands are resonantly excited vibrational states of $\tilde{C}(4\sigma_g^{-1})$. Given this tentative conclusion, we propose assignments for the new peaks in Table I. In making these assignments, the issue of the ν_3 vibrational frequency becomes critical. We find that the numerous vibrational states evidenced in Table I are difficult to ascribe with any other assignment (001, 002, or 011) than (101) for the band at 19.755 eV binding energy. The (101) assignment yields a ν_3 vibrational frequency of 193 meV, which is close to that for the $\tilde{X}$ state (182 meV).[30,58] Our assignment is further supported by recent molecular beam photoelectron work, which reports a ν_3 frequency of 1567(4) cm^{-1} (194 meV)[31] as well as by other considerations mentioned earlier.

Photoelectron spectra measured at four different photon energies in the resonant region are presented in Fig. 3. They illustrate how strongly resonant the new peaks are in the narrow 23–24-eV photon-energy range. The branching ratio with respect to (000) of the most prominent resonant band at 19.634 eV binding energy is shown in Fig.4. Note that the relative intensity on resonance at 23.4 eV is more than 10 times higher than that off resonance. The other vibrational states [except for (000)], as well as the (101) band, all clearly demonstrate resonant behavior in the 23–24-eV range, as shown in Figs. 5 and 6. Figures 5 (top) and 7 show asymmetry parameters for the $\tilde{C}$ state bands (000), unresolved (100 + 020), and (101) in the 20 to 28-eV range. The position of the sharp resonance in the branching ratio of the $\tilde{C}(100 + 020)$ band (Fig. 5, bottom) corresponds to a rapid change in the β parameter (Fig. 5, top).

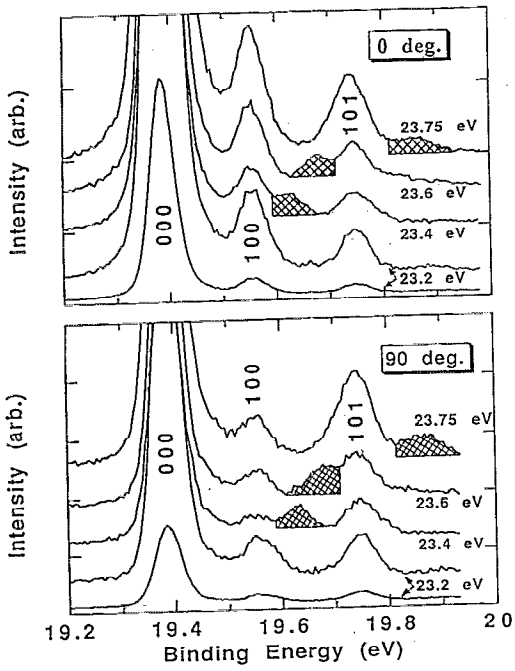

FIG. 3. Photoelectron spectra illustrating the appearance of bands at 19.634, 19.685, and 19.87 eV binding energy (see cross-hatched peaks). Spectra have been measured at $\theta = 0°$ (top) and 90° (bottom) and with photon energies of 23.2, 23.4, 23.6, and 23.75 eV (from bottom to top in each panel). The spectral intensities have been scaled arbitrarily for purposes of comparison.

It is difficult to assign the resonances responsible for the appearance of the many new peaks. For these photon energies, no high-resolution absorption measurements on CO_2 are available; the total ionization cross section of Brion and Tan[35] does not present structures between 23 and 24 eV, although their resolution of about 1 eV would probably smear out any weak, sharp structures. However, the observation of satellites at binding energies of 22.7, 25.1, and 27.3 eV[57,59–61] implies the presence of Rydberg series converging to these states. We tentatively conclude that these doubly excited Rydberg states are the origin of the observed resonant behavior.

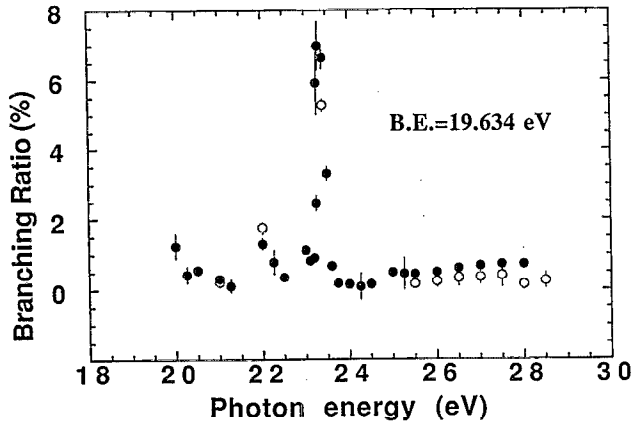

FIG. 4. Branching ratio relative to the $\tilde{C}(000)$ band of the peak at 19.634 eV binding energy (suggested assignment 110). Filled circles are from $5V$ pass spectra; open circles are from $2V$ pass spectra.

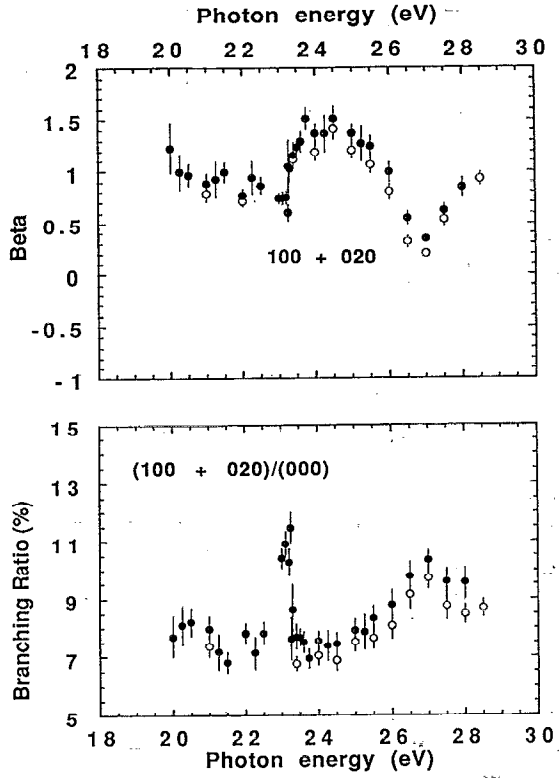

FIG. 5. (Top) Energy dependence of the β for the unresolved $\tilde{C}(100 + 020)$ bands in the $h\nu = 20$–28.5 eV range. (Bottom) Branching ratio relative to the $\tilde{C}(000)$ main band of the unresolved $\tilde{C}(100 + 020)$ bands. Filled circles are from $5V$ pass spectra; open circles are from $2V$ pass spectra.

B. Continuum–continuum coupling

The β of the $\tilde{C}(000)$ band contains two broad minima at 22 and 28 eV photon energy (Fig. 7), in addition to the well-known dip near 40 eV (outside the range of our results) assigned to a shape resonance in the $\varepsilon\sigma_u$ continuum.[37–45] No structures have been predicted in the 20–30-eV range for photoionization of the $4\sigma_g$ orbital into the $\varepsilon\pi_u$ or $\varepsilon\sigma_u$ continuum channels. However, all previous calculations neglect

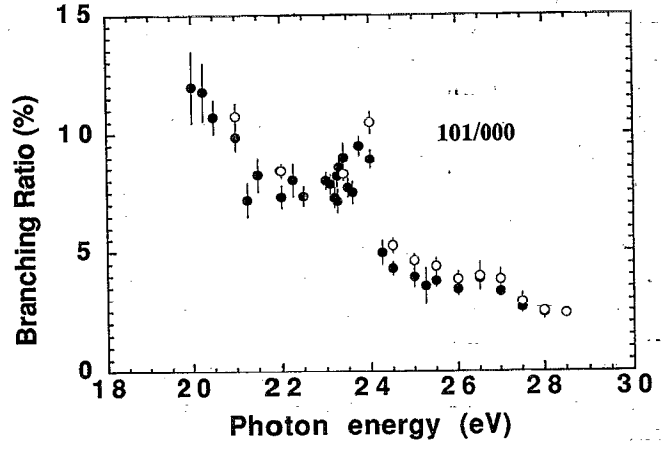

FIG. 6. Branching ratio of the $\tilde{C}(101)$ band relative to the $\tilde{C}(000)$ band. Filled circles are from $5V$ pass spectra; open circles are from $2V$ pass spectra.

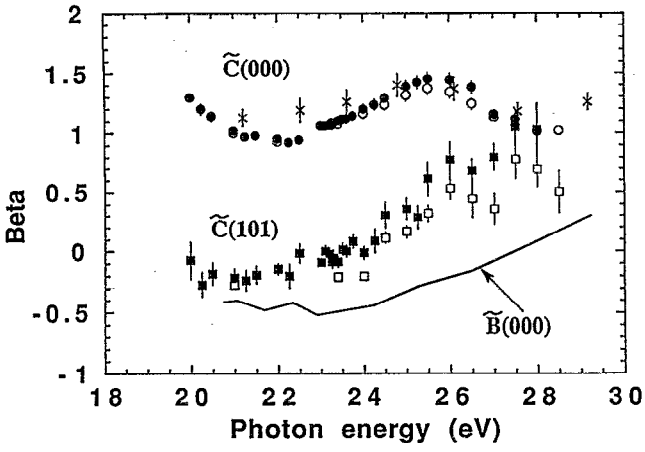

FIG. 7. β for the $\tilde{C}(000)$ [circles], $\tilde{C}(101)$ [squares], and $\tilde{B}(000)$ [solid line] bands. Filled symbols are from $5V$ pass spectra; open symbols are from $2V$ pass spectra. For the $\tilde{B}(000)\beta$, the line connects experimental results of Grimm *et al.*,[34] which have been shifted to be on the same *kinetic* energy scale as the $\tilde{C}(101)$ data. The X symbol represents experimental data taken from Grimm *et al.*[34] for the $\tilde{C}(000)$ band.

coupling between different electronic continua, i.e., continuum–continuum coupling. Such coupling is usually weak because continuum electrons are so diffuse that they have negligible amplitude in the molecular interior. Shape resonances provide a mechanism for trapping the electron in the molecular core, resulting in enhancement of interchannel coupling.[47] For example, theoretical studies[47,48] of N_2 show that after incorporating continuum–continuum coupling, the β curve for $2\sigma_u^{-1}$ ionization shows a resonant feature transferred from the $3\sigma_g^{-1}$ channel, where a shape resonance exists at $h\nu = 29$–30 eV. Experimental data[46,61] on the $2\sigma_u^{-1}$ channel show a systematic deviation from the one-electron calculations in accordance with this prediction.

For CO_2, shape resonances have been predicted[34,39–41,45] in the $\varepsilon\sigma_g$ and $\varepsilon\pi_g$ continua for the $3\sigma_u^{-1}$ $\tilde{B}\,^2\Sigma_u^+$ ionization channel at about $h\nu = 21$ and 40 eV, respectively. The effects of the low energy $\varepsilon\sigma_g$ resonance are quite prominent, both in the partial cross section and in the β curve; however, the high-energy $\varepsilon\pi_g$ resonance is much broader, and the effects are predicted to be much weaker. In the context of the present measurement, we note that the β for the $3\sigma_u^{-1}$ $\tilde{B}\,^2\Sigma_u^+$ channel exhibits a prominent dip at $h\nu \sim 21$ eV, for which experiment and theory are in good agreement. The β has not been measured in the range $h\nu = 28$–40 eV, where the calculations predict a plateau or faint dip beginning at $h\nu = 28$–30 eV, depending upon the calculation. On the basis of the example[46–48] of continuum–continuum coupling between the $2\sigma_u^{-1}$ and $3\sigma_g^{-1}$ channels of N_2, we note the possibility that the dip at $h\nu \sim 22$ eV that we observe in the β curve for the $\tilde{C}(000)$ band (Fig. 7) results from continuum–continuum coupling between the $4\sigma_g^{-1}$ and $3\sigma_u^{-1}$ channels of CO_2. This, of course, is a highly speculative interpretation which requires calculations of the shape-resonance-induced coupling strength to assess its plausibility. Owing to the weakness of the effects of the $\varepsilon\pi_g$ resonance in the calculated β curve for the $3\sigma_u^{-1}$ $\tilde{B}\,^2\Sigma_u^+$ channel, unusually strong coupling would be required to cause the dip we see in the β for $\tilde{C}(000)$ at $h\nu \sim 28$ eV; therefore, similar speculation regarding this feature seems unwarranted. Finally, we note that similar minima at approximately the same energies occur in the β curve for the $\tilde{C}(100)$ band (Fig. 5, top), suggesting that similar effects arise in both the $\tilde{C}(000)$ and $\tilde{C}(100)$ band. We hope that such observations will stimulate vibrationally resolved calculations including continuum–continuum coupling for these channels in CO_2.

C. Vibronic coupling

The $\tilde{C}(010)$ band is too weak and unresolved from the $\tilde{C}(000)$ band in the present measurement to allow a precise determination of its branching ratio and β parameter. We estimate its intensity to be 5(2)%, relative to the $\tilde{C}(000)$ band, in the energy range considered here, except possibly near the sharp resonances at 23–24 eV. A higher resolution study would be warranted to determine the origin of this symmetry-forbidden band, which is likely to be caused by vibronic coupling with the $\tilde{A}\,^2\Pi_u$ $(n00)$ states, as discussed above.

The main object of this study is the $\tilde{C}(101)$ band at 19.755 eV binding energy, which we and others have concluded arises from vibronic coupling with the $\tilde{B}\,^2\Sigma_u^+$ state. Figure 7 presents new evidence for this mechanism in the form of the wavelength dependence of the photoelectron angular distribution for the $\tilde{C}(000)$, $\tilde{C}(101)$, and $\tilde{B}(000)$ levels. There it is very clear that the $\tilde{C}(101)$ band behaves very differently from the $\tilde{C}(000)$ band of the same electronic state and very similarly to the $\tilde{B}(000)$ band. Mechanistically, this result suggests that, as the photoionization of the $3\sigma_u^{-1}$ orbital of CO_2 proceeds, vibronic coupling will induce a small fraction of the $\tilde{B}\,^2\Sigma_u^+$ (000) residual ion states to convert to $\tilde{C}\,^2\Sigma_g^+$ (101) states, with the concomitant change in the asymptotic kinetic energy and symmetry in the ejected photoelectrons. So, although these photoelectrons exhibit a kinetic energy characteristic of the $\tilde{C}\,^2\Sigma_g^+$ (101) state of the ion, they also carry dynamical information characteristic of the $3\sigma_u^{-1}$ channel from which the photoionization intensity is being borrowed.

The branching ratio of the $\tilde{C}(101)$ band relative to the $\tilde{C}(000)$ band also offers some support for this interpretation. As seen in Fig. 6, the $\tilde{C}(101)$ strength decreases monotonically relative to the $\tilde{C}(000)$, suggesting that the strength of the forbidden $\tilde{C}(101)$ arises from an origin other than simple $4\sigma_g^{-1}$ photoionization, which of course it must since it is forbidden. Partial cross section data by Brion and Tan[35] reflect the same qualitative behavior for the $\tilde{B}$ state, further suggesting the role of this state in the formation of the $\tilde{C}(101)$ band.

V. CONCLUSIONS

High-resolution triply differential photoelectron studies of the $\tilde{C}$ state of CO_2^+ have provided new and detailed information about the spectroscopy and the complex dynamics associated with ionization from the $4\sigma_g$ orbital. First, in addition to the bands previously observed, our photoelectron spectra reveal resonantly excited vibrational levels, which

helped to confirm the ν_3 frequency of 193 meV (1557 cm^{-1}) for the $\tilde{C}$ state. Their strongly resonant behavior in a narrow energy range suggests autoionization of doubly excited states as the origin of their intensity. Second, the β for the $\tilde{C}(000)$ and $\tilde{C}(100)$ bands over the photon energy range 20–38 eV are suggestive of continuum–continuum coupling between the $4\sigma_g^{-1}\,\tilde{C}\,^2\Sigma_g^+$ and the $3\sigma_u^{-1}\,\tilde{B}\,^2\Sigma_u^+$ ionization channels.

Most importantly, our β and branching ratio measurements of the forbidden $\tilde{C}(101)$ level strongly support the role of vibronic coupling as discussed by Domcke.[20] In fact, both the $\tilde{C}(101)$ and the $\tilde{B}(000)$ bands have generally similar β curves and intensity variations in this energy range. This was the first study in which the energy dependence of photoelectron angular distributions and vibrational branching ratios were used to demonstrate vibronic coupling by observing the dynamical signature of the state from which the forbidden band borrows its intensity. Vibronic coupling is a general and widespread phenomenon in molecular spectra; and, although higher resolution than that employed here will be required in many cases, we believe that this approach will become very useful in establishing the nature of complex vibronic manifolds as synchrotron-based photoelectron spectrometers improve.

ACKNOWLEDGMENTS

Experiments were performed at the National Institute of Standards and Technology (NIST) synchrotron storage ring (SURF). We thank the SURF staff for their help and cooperation in the delivery of many hours of "low fuzz" beam. We also wish to acknowledge useful suggestions from Dr. E. Poliakoff regarding the discussion of continuum–continuum coupling. This work was supported in part by the U.S. Department of Energy, Assistant Secretary for Energy Research, Office of Health and Environmental Research, under Contract W-31-109-Eng-38 and in part by the Los Alamos National Laboratory Physics Division. One of us (V.S.) wishes to thank the Photon Physics group at NIST for their kind hospitality and the National Institute of Standards and Technology and the Deutsche Forschungsgemeinschaft for financial assistance.

[1]V. McKoy, T. A. Carlson, and R. R. Lucchese, J. Phys. Chem. **88**, 3188 (1984).
[2]J. L. Dehmer, A. C. Parr, and S. H. Southworth, in *Handbook on Synchrotron Radiation*, edited by G. V. Marr (North-Holland, Amsterdam, 1987), Vol. II, Chap. 5, p. 241.
[3]I. Nenner and J. A. Beswick, in *Handbook on Synchrotron Radiation*, edited by G. V. Marr (North-Holland, Amsterdam, 1987), Vol. II, Chap. 6, p. 355.
[4]G. Herzberg, in *Electronic Spectra and Electronic Structure of Polyatomic Molecules* (D. Van Nostrand Co., Princeton, NJ, 1966).
[5]J. L. Dehmer, D. Dill, and S. Wallace, Phys. Rev. Lett. **43**, 1005 (1979).
[6]J. B. West, A. C. Parr, B. E. Cole, D. L. Ederer, R. Stockbauer, and J. L. Dehmer, J. Phys. B **13**, L105 (1980).
[7]R. R. Lucchese and V. McKoy, J. Phys. B **14**, L629 (1981).
[8]G. Herzberg and Ch. Jungen, J. Mol. Spectrosc. **41**, 425 (1972).
[9]P. M. Dehmer and W. A. Chupka, J. Chem. Phys. **65**, 2243 (1976).
[10]M. Raoult and Ch. Jungen, J. Chem. Phys. **74**, 3388 (1981).
[11]S. Krummacher, V. Schmidt, and F. Wuilleumier, J. Phys. B **13**, 3993 (1980).
[12]S. Krummacher, V. Schmidt, F. Wuilleumier, J. M. Bizau, and D. Ederer, J. Phys. B **16**, 1733 (1983).
[13]L. S. Cederbaum and W. Domke, Adv. Phys. Chem. **36**, 205 (1977).
[14]G. Wendin, *Structure and Bonding* (Springer, Berlin, 1981), Vol. 45.
[15]H. Koppel, W. Domcke, and L. S. Cederbaum, in *Advances in Chemical Physics*, edited by I. Prigogine and S. A. Rice (Wiley/Interscience, New York, 1984), Vol. 57, p. 59.
[16]T. A. Carlson, Chem. Phys. Lett. **9**, 23 (1971).
[17]T. A. Carlson and A. E. F. Jonas, Chem. Phys. **55**, 5913 (1971).
[18]T. A. Carlson, G. E. McGuire, A. E. Jonas, K. L. Cheng, C. P. Anderson, C. C. Lu, and B. P. Pullen, in *Electron Spectroscopy*, edited by D. A. Shirley (North Holland, Amsterdam, 1972).
[19]T. A. Carlson and G. E. McGuire, J. Electron Spectrosc. **1**, 209 (1972).
[20]W. Domcke, Phys. Scr. **19**, 11 (1979).
[21]A. C. Parr, S. H. Southworth, J. L. Dehmer, and D. M. P. Holland, Nucl. Instrum. Methods **222**, 221 (1984).
[22]D. L. Ederer, B. E. Cole, and J. B. West, Nucl. Instrum. Methods **172**, 185 (1980).
[23]See, for example, V. G. Horton, E. T. Arakawa, R. N. Hamm, and M. W. Williams, Appl. Opt. **8**, 667 (1969).
[24]S. H. Southworth, A. C. Parr, J. E. Hardis, J. L. Dehmer, and D. M. P. Holland, Nucl. Instrum. Methods **246**, 782 (1986).
[25]C. R. Brundle and D. W. Turner, Int. J. Mass Spectrosc. Ion Phys. **2**, 195 (1969).
[26]J. H. D. Eland and J. Berkowitz, J. Chem. Phys. **67**, 2782 (1977).
[27]A. W. Potts and G. H. Fattahallah, J. Phys. B **13**, 2545 (1980).
[28]I. Reineck, C. Nohre, R. Maripuu, P. Lodin, S. H. Al-Shamma, H. Veenhuizen, L. Karlsson, and K. Siegbahn, Chem. Phys. **78**, 311 (1983).
[29]B. Kovac, J. Chem. Phys. **78**, 1684 (1983).
[30]H. Veenhuizen, B. Wannberg, L. Mattsson, K.-E. Norell, C. Nohre, L. Karlsson, and K. Siegbahn, J. Electron Spectrosc. **41**, 205 (1986).
[31]L. S. Wang, J. E. Ruett, Y. T. Lee, and D. A. Shirley, J. Electron Spectrosc. **47**, 167 (1988).
[32]T. Baer and P. M. Guyon, J. Chem. Phys. **85**, 4765 (1986).
[33]J. Kreile and A. Schweig, J. Electron Spectrosc. **20**, 191 (1980).
[34]F. A. Grimm, J. D. Allen, Jr., T. A. Carlson, M. O. Krause, D. Mehaffy, P. R. Keller, and J. W. Taylor, J. Chem. Phys. **75**, 92 (1981).
[35]C. E. Brion and K. H. Tan, Chem. Phys. **34**, 141 (1978).
[36]T. A. Carlson, M. O. Krause, F. A. Grimm, J. D. Allen, Jr., D. Mehaffy, P. R. Keller, and J. W. Taylor, Phys. Rev. A **23**, 3316 (1981).
[37]P. Roy, I. Nenner, M. Y. Adam, J. Delwiche, M. J. Hubin-Franskin, P. Lablanquie, and D. Roy, Chem. Phys. Lett. **109**, 607 (1984).
[38]P. Roy, Ph.D. thesis, Universite Laval, Quebec, Canada, Dec. 1986.
[39]F. A. Grimm, T. A. Carlson, W. B. Dress, P. Agron, J. O. Thomson, and J. W. Davenport, J. Chem. Phys. **72**, 3041 (1980).
[40]N. Padial, G. Csanak, B. V. McKoy, and P. W. Langhoff, Phys. Rev. A **23** 218 (1981).
[41]J. R. Swanson, D. Dill, and J. L. Dehmer, J. Phys. B **14**, L207 (1981); **13**, L231 (1980). The $\varepsilon\sigma_g$ resonance in the $3\sigma_u^{-1}$ channel at $h\nu\sim20$ eV was mislabeled $\varepsilon\pi_g$ in the first of these papers. It was correctly described in an extended version of this paper in Ref. 45.
[42]R. R. Lucchese and V. McKoy, Phys. Rev. A **26**, 1406 (1982).
[43]R. R. Lucchese and V. McKoy, Phys. Rev. A **26**, 1992 (1982).
[44]L. A. Collins and B. I. Schneider, Phys. Rev. A **29**, 1695 (1984).
[45]P. M. Dittman, D. Dill, and J. L. Dehmer, Chem. Phys. **78**, 405 (1983).
[46]S. H. Southworth, A. C. Parr, J. E. Hardis, and J. L. Dehmer, Phys. Rev. A **33**, 1020 (1986).
[47]J. A. Stephens and D. Dill, Phys. Rev. A **31**, 1968 (1985).
[48]B. Basden and R. R. Lucchese, Phys. Rev. A **37**, 89 (1988).
[49]Y. Tanaka, A. S. Jursa, and F. J. LeBlanc, J. Chem. Phys. **32**, 1199 (1960).
[50]Y. Tanaka and M. Ogawa, Can. J. Phys. **40**, 879 (1962).
[51]G. R. Cook, P. H. Metzger, and M. Ogawa, J. Chem. Phys. **44**, 2935 (1966).
[52]K. E. McCulloh, J. Chem. Phys. **59**, 4250 (1973).
[53]M. S. Hubin-Franskin, J. Delwiche, P. Morin, M. Y. Adam, I. Nenner, and P. Roy, J. Chem. Phys. **81**, 4246 (1984).

[54]F. A. Grimm and M. Larsson, Phys. Scr. **29**, 337 (1984).
[55]T. Gustafsson, E. W. Plummer, D. E. Eastman, and W. Gudat, Phys. Rev. A **17**, 175 (1978).
[56]C. J. Allan, U. Gelius, D. A. Allison, G. Johanson, H. Siegbahn, and K. Siegbahn, J. Electron Spectrosc. **1**, 131 (1972/73).
[57]F. P. Larkins and J. A. Richards, Aust. J. Phys. **39**, 1 (1986); T. A. Ferrett, D. W. Lindle, P. A. Heimann, W. D. Brewer, U. Becker, H. G. Kerkhoff, and D. A. Shirley, Phys. Rev. A **36**, 3172 (1987).
[58]M. A. Johnsson, R. N. Zare, J. Rostas, and S. Leach, J. Chem. Phys. **80**, 2407 (1984).
[59]H. J. Freund, H. Kossmann, and V. Schmidt, Chem. Phys. Lett. **123**, 463 (1986).
[60]P. Roy, I. Nenner, P. Millie, P. Morin, and D. Roy, J. Chem. Phys. **84**, 2050 (1986).
[61]G. V. Marr, J. M. Morton, R. M. Holmes, and D. G. McCoy, J. Phys. B **12**, 43 (1979).